

EFFECT OF SPANWISE BLOWING IN THE ANGLE-OF-ATTACK REGIME $\alpha = 0 + 90^\circ$ *

W. Staudacher, B. Laschka
Messerschmitt-Bölkow-Blohm GmbH
München-Ottobrunn, W-Germany

Ph. Poisson-Quinton, J.P. Ledy
O.N.E.R.A.
Paris-Chatillon, France

ABSTRACT

This report summarizes results of experimental investigations conducted in the course of a Franco-German cooperation, the aim of which is to find out the benefits of spanwise blowing at subsonic speeds and high angles of attack.

Aerodynamic and system-integrated effects due to concentrated spanwise blowing are demonstrated regarding

- o stability and control
- o high lift performances and boundaries

for a basic fighter-type pilot model.

In a first step the position of the blowing jet was optimized relative to the wing upper surface.

Configurational items were considered such as

- o clean wing
- o strake wing
- o high lift configuration

In a second step the angle of attack regime investigated was extended up to 90° for the selected strake-wing configuration.

Analysis of the results shows marked improvements of aerodynamic characteristics utilizing concentrated spanwise blowing, which proves to be powerful and simple means to increase maneuver performances at high angles-of-attack.

I. INTRODUCTION

Spanwise blowing was originally introduced to improve the high-lift (high angle-of-attack) capabilities of (fighter type) aircraft. Hence this technique has to be seen in the light of the contradictory claims made on a fighter wing which arise from the requirements for good low speed and transonic/supersonic performances and flying qualities as well.

Satisfying this compromise in a modern way hybrid wing planforms or strake wings were developed (F16, F17, F18). These wings draw their superiority at high

angles-of-attack from the existence of strong, separated leading edge vortices shedding from the sharp noses of the slender highly swept strakes. This type of generating concentrated stable vortex systems is thus based on planform items and profile characteristics.

To generate similar beneficial, non-linear aerodynamic effects on arbitrary planforms, transversal or spanwise concentrated blowing is used, which then induces analogous improvements i.e. non-linear increase of lift with a.o.a. and consequently reduced lift-dependent drag for near zero-leading-edge-suction conditions.

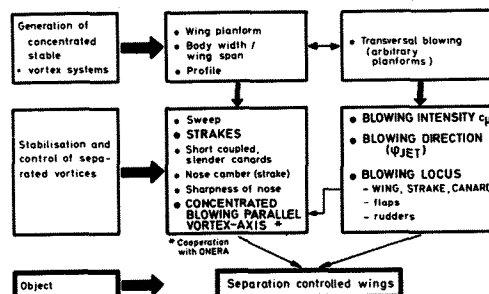


FIG.1 Working Group
"WINGS WITH CONTROLLED SEPARATION":
GENERAL APPROACH
(MEMBERS: DFVLR, VFW-FOKKER, MBB)

This coincides with the scope of investigations carried out by a working group named "Wings With Controlled Separation", which is sponsored by the German M.o.D. Members are research engineers of DFVLR, MBB and VFW-F.

Fig. 1 shows the general approach taken by this group to generate and/or stabilize and control separated vortices with the objective of developing "Separation Controlled Wings". The parameters and devices listed in Fig. 1 were all investigated. This paper is concerned with the items printed in fat letters and hence will present combined and selected effects of strakes and/or spanwise blowing. The extension of this technique to extreme angles-of-attack was done in cooperation with O.N.E.R.A.

* This research was supported by the German Ministry of Defence

Before presenting details of the research programme some justification for application of spanwise blowing in the aforementioned sense has to be given. Fig. 2 shows the approximate "state of the art" for the maneuver boundaries of a typical fighter aircraft as derived from the experimental programme described above. The possible regions of application of spanwise blowing are denoted with numbers ① to ④.

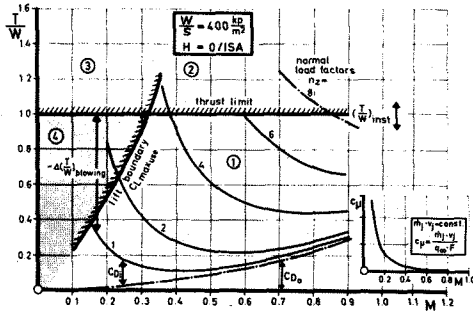


FIG. 2 MANEUVER BOUNDARIES FOR A TYPICAL FIGHTER CONFIGURATION AND REGIONS OF APPLICATION OF SPANWISE BLOWING

For a wing loading $W/S = 400 \text{ kp/m}^2$, $H = 0 / \text{ISA}$ drag curves for different normal load factors are plotted versus Mach numbers. For stationary maneuvers an upper limit is defined by the intersection of the n_z -curves with the nominal thrust/weight ratio, here assumed $T/W = 1.0$ (thrust or drag boundary).

In the low speed regime the lift boundary $C_{Lmaxuse}$ becomes decisive. Hence we can separate four regions, defined by the intersection of the boundaries.

- ① limited by thrust or lift; spanwise blowing is applicable but we shall find drastic reduced c_{Dj} -values with increasing M-number, see insert chart $c_{Dj}(M)$ for constant $m_j \cdot v_j$
- ② thrust limited; no "thrust reserves" for spanwise blowing
- ③ thrust and lift limited
- ④ lift limited, excess thrust for spanwise blowing available.

Hence, as spanwise blowing is known to be a non-linear technique, extending the lift boundary as well as the angle-of-attack of maximum lift, but not restoring L.E. suction (as BLC methods tend to do thus shifting the drag curves down), the low speed region ④ is the primary field for application of spanwise blowing.

Nevertheless there are possible applications of this technique in transonics as demonstrated in the next paper by DIXON, DANSBY and POISSON-QUINTON.

II. EXPERIMENTAL PROGRAMME

The first part of the experimental programme was directed towards the optimisation of the blowing locus for different configurations. The tests were carried out in the 3 x 3m low speed tunnel of DFVLR Göttingen and were restricted to angles-of-attack $\alpha \leq 30^\circ$ due to model size and blockage reasons. The configurations and parameters investigated are schematically sketched in Fig. 3.

The position of the blowing jet relative to the respective wing upper surface was varied by different nozzle locations

- o 3 chordwise positions ($x_D/c_r = 0.10/0.25/0.40$)
- o 3 nozzle heights ($z_D/d = 1.0/1.5/2.0$)
- o 4 nozzle sweep angles ($\Delta\phi_D = 5^\circ/10^\circ/15^\circ/18^\circ$)

$\Delta\phi_D$ is defined as incremental sweep of the nozzle axis relative to the sweep of the respective constant % chord line, positive aft.

Comparison of Configurations for $c_{Dj} = \text{const.}$			Results
			①, ② Optimum Nozzle Position (x_D/c_r) ③ Optimum Jet Direction (ϕ_D)
			Blowing Efficiency Stroke on/off ④ Flap, Stroke on/off ④, ⑤ Optimum Blowing Position ⑥-⑦-⑧? Interference of Vortex Systems
			⑦, ⑧ Optimum Nozzle Position ⑨ Optimum Jet Direction Flap ⑩, ⑪ Effect of Gap ⑩-⑪-⑫? Interference of Vortex Systems
			Blowing Efficiency Stroke on/off ⑩, ⑪ Optimum Blowing Position ⑩-⑪-⑫? Interference of Vortex Systems
	Flaps "above Wing" (KASPER Concept) Gap sealed/rear		a. without Blowing (Re-Variation) b. with Blowing • Effect of Gap • Jet Location • Blowing over Flap • Blowing over Wing • Blowing over Flap and Wing

FIG. 3 CONFIGURATIONS AND PARAMETERS INVESTIGATED

The nozzle position on the strake wing was at 10% root chord of the strake wing with axis parallel to the strake L.E. (75° , see point ⑤). Simultaneous blowing on two chordwise positions was possible. Basic and strake wing configurations were tested clean as well as with high-lift flaps applied. Additionally a flap system "above the wing" (so-called KASPER-concept) was studied.

The second part of the experimental programme was directed towards the investigation of the effects of spanwise blowing at extreme angles-of-attack $\alpha = 0 + 90^\circ$. These tests were carried out in the $\phi = 8\text{m}$ tunnel S1 ONERA Modane in the course of a

scientific cooperation with O.N.E.R.A. Primary objective of this phase was to find out the effects on performance, stability and control and, last not least, on buffet- and departure-characteristics at these extreme incidences.

III. MODEL AND APPARATUS

All the tests were executed with the MBB Low Speed Pilot Model, which is sketched in Fig. 4 (top), using the basic wing ① defined by an aspect ratio $AR = 3.2$, leading edge sweep $\Lambda_{LE} = 32^\circ$ and a taper ratio $\lambda = 0.3$.

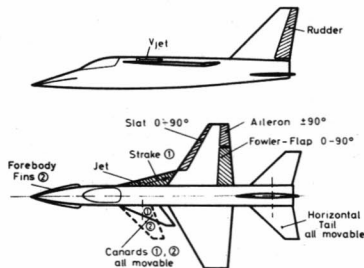


FIG. 4 PILOT MODEL

The wing is twisted and cambered. Wing modifications consisted of a maneuver flap system (L.E. slats and T.E. single-slotted fowler flaps) and detachable strakes, which could be replaced by canards of identical exposed area (11% of basic wing reference area). The strake ① under consideration here has a straight L.E. of 75° sweep. Conventional controls as rudder, ailerons and taileron were used, with extended range of deflections.

The photo in Fig. 4 (bottom) shows a side view of the pilot model mounted in the 3 x 3 m L.S. tunnel of DFVLR Göttingen. The different chordwise positions of the nozzles are evident: the most forward position used when the strake is attached, 3 positions above the basic wing (10/25/40% root chord) and one position at 25% flap chord, when the flap is deflected 30° as shown in the photo. The nozzles are housed in a fibre-glass fairing. Two sets of nozzles were available: exit diameter 15 mm ($\hat{=} 2.6\% c_r$) and 7.5 mm ($\hat{=} 1.3\% c_r$).

The convergent nozzles were usually driven with supercritical pressure ratio. The blowing system was sting mounted and so arranged force free within the model; by that, mere aerodynamic, induced effects of spanwise blowing were measured.

IV. RESULTS

IV. 1. Optimization of Jet Position and Direction

This chapter is concerned with the conventional angle-of-attack regime $\alpha \leq 30^\circ$, and all the tests were executed in the 3 x 3 m L.S. tunnel of DFVLR Göttingen at Re-Numbers of $\sim 2.0 \cdot 10^6$.

IV. 1.1 Basic clean wing without strake

As already noted in Fig. 3 the optimum position of the nozzle was found varying the chordwise location x_D/c_r , nozzle axis height above the wing z_D/d and jet sweep φ_D , for a constant supercritical blowing coefficient $c_{\mu} = 0.1$. The criterion used is the maximum lift increment ΔC_{Lmax} induced by spanwise blowing.

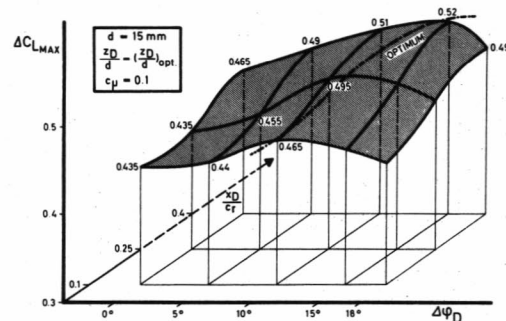


FIG. 5 OPTIMIZATION OF JET POSITION AND DIRECTION

In Fig. 5 part of the optimization process is plotted for constant nozzle height, varying chordwise position and jet sweep angle.

Optimum position is defined by

- o chordwise position at 40% root chord
- o nozzle height 1.5ϕ
- o blowing direction $\varphi_D \approx \Lambda_{LE}$
($\Delta\varphi_D = 15^\circ =$ blowing approximately parallel to wing leading edge)

Nozzle height was found to be the most insensitive parameter in this range investigated ($z_D/d = 1.0 + 2.0$).

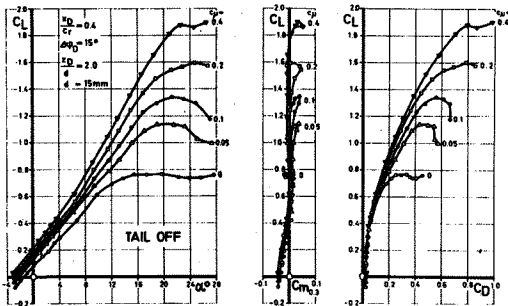


FIG. 6 EFFECTS OF SPANWISE BLOWING ON LIFT, PITCHING MOMENT AND DRAG (STRAKE OFF)

Fig. 6 gives the influence of increased blowing intensity c_{μ} on the development of lift, pitching moment and drag.

Dominant effects are

- o increase of maximum lift with simultaneous increase of angle of attack of maximum lift
- o linearized pitching moment without significant changes in zero-lift moment and neutral point position
- o reduced lift dependent drag at high incidences

Drag is further analysed in Fig. 7a, b.

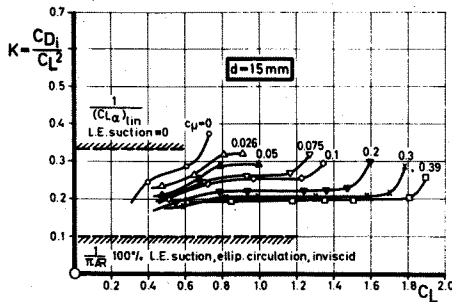


FIG. 7a ANALYSIS OF DRAG AS AFFECTED BY SPANWISE BLOWING (BASIC WING, STRAKE OFF)

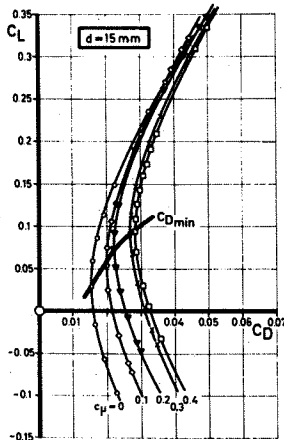


FIG. 7b ANALYSIS OF DRAG AS AFFECTED BY SPANWISE BLOWING (BASIC WING, STRAKE OFF)

At high lift coefficients lift-dependent drag is drastically reduced by increased blowing coefficients c_{μ} as demonstrated in Fig. 7a by the induced drag factor K . A "plateau" is developing, which is shifted to lower K -values and extended to higher lift coefficients with increasing c_{μ} . The curve for $c_{\mu} = 0.1$ gives a similar trend as found for the strake wing without blowing.

Fig. 7b shows that there is an increase in the minimum drag level CD_{min} due to spanwise blowing. This is an analogon to the quasi-camber effect already found in Fig. 6 for the lift curves, which are shifted parallel at low incidences, similar as flap deflections tend to do. This "camber-effect" was not found in the pitching moment curves (constant center of pressure for varying jet coefficients c_{μ}).

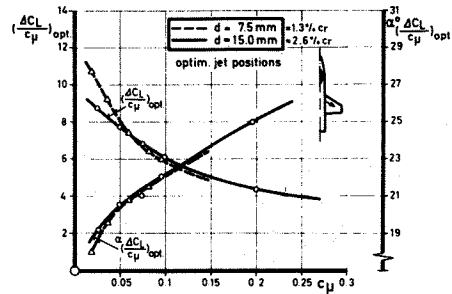


FIG. 8 BLOWING EFFICIENCY ON CLEAN BASIC WING CONFIGURATION EFFECT OF c_{μ} AND NOZZLE DIAMETER

Dividing the jet-induced lift increment by the inducing jet coefficient gives an efficiency factor $\Delta CL/c_{\mu}$ of the technique, relative to the effect of a hovering jet ($\Delta CL/c_{\mu} = 1$).

In Fig. 8 this aerodynamic amplification factor $\Delta CL/c_{\mu}$ is plotted versus c_{μ} for optimum angles-of-attack and two different nozzle diameters. It is well known, that supercritically driven blowing jets are more effective in producing additional lift. Hence the smaller nozzle ($\phi = 7.5$ mm) is more effective at low c_{μ} -values than the ($c_{\mu} < 0.08$) still subcritical working big nozzle ($\phi = 15$ mm).

IV. 1.2 Clean Strake Wing

For the strake configuration the nozzle locations investigated are the same as for the basic wing with an additional position at 10% root chord of the strake wing (see Fig. 3 and Fig. 5). The possibility of combined blowing exists (simultaneously working nozzles on the strake and the basic wing).

The superior jet position found was that blowing on the strake parallel to the leading edge at a nozzle height of 1.5ϕ above the wing surface.

Similar trends as resulting for the basic wing are found for lift, drag and pitching moment of the strake wing (Fig. 9).

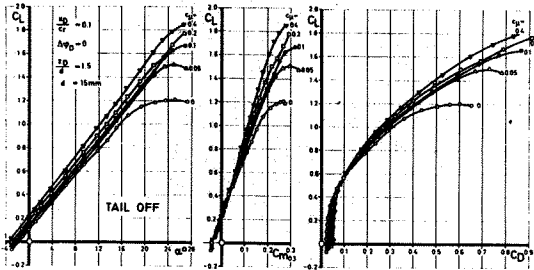


FIG. 9 EFFECTS OF SPANWISE BLOWING ON LIFT, PITCHING MOMENT AND DRAG (OPTIMUM NOZZLE POSITION, STRAKE ON)

Generally, the lift increase and consequently drag reduction due to spanwise blowing on the strake wing is reduced, compared to the data for the basic wing without strake. This can be traced back to the higher level of nonlinearity already inherent to the strake configuration without blowing. On the other side the effect of linearizing the pitching moment curves is more pronounced on the strake wing (reduction of pitch-up tendency of this configuration).

A comparison of the efficiency of spanwise blowing on the clean basic and strake wing is given in Fig. 10.

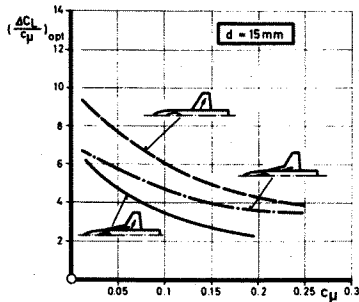


FIG. 10 EFFECT OF JET LOCATIONS ON BLOWING EFFICIENCY (CLEAN CONFIGURATIONS)

Combined blowing was found to be the inferior technique. As expected, stabilization of the existing strake vortex system proved to be more difficult and less effective.

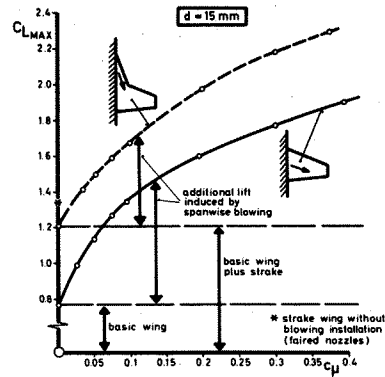


FIG. 11 SUMMARY OF LIFT PRODUCING EFFECT OF SPANWISE BLOWING ON BASIC AND STRAKE WING

In Fig. 11 a summary of the maximum lift build-up due to spanwise blowing on the basic and strake wing is presented.

The data for the strake wing are extrapolated for $c_{\mu} \geq 0.2$ and are regarded too optimistic.

IV. 1.3 High-Lift Configurations

Fig. 12 compares the blowing efficiency on the basic and strake wing, high-lift flap system extended.

Blowing on the basic wing in high-lift configuration gave the overall highest efficiency found in the investigation. Two examples for contemporary fighters, which apply boundary layer control either on the trailing edge or on the leading edge flap, are shown additionally. Even if the efficiency of both techniques is at the same level for this criterion $\Delta C_L / c_{\mu}$ one should keep in mind that BLC techniques increase the flap effectiveness and thus reduce angle-of-attack for a given lift coefficient, whilst the non-li-

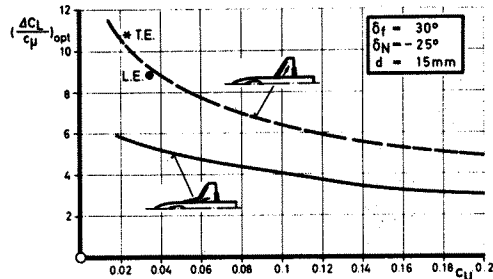


FIG. 12 BLOWING EFFICIENCY ON HIGH LIFT CONFIGURATION (*, • BLC ON CONTEMPORARY FIGHTERS)

near additional lift due to spanwise blowing is produced at increasing angles-of-attack (analogous to the effect of the strake).

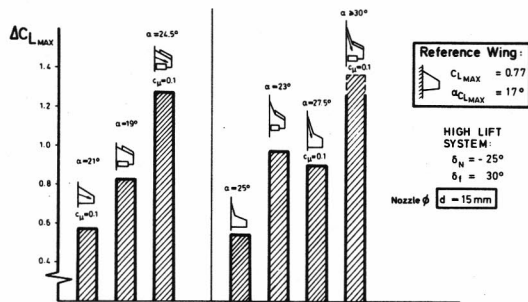


FIG. 13 SPECIFIC AND COMBINED EFFECTS OF SPANWISE BLOWING, STRAKE AND HIGH LIFT FLAP SYSTEM

In Fig. 13 the specific and combined effects of spanwise blowing and/or strake and/or flap system are compared. Again the criterion is the maximum lift increment. All increments are given relative to the clean, unblown basic wing = reference wing. As can be easily seen, the blown clean basic wing ($c_{\mu} = 0.1$) gives about the same lift as the unblown, clean strake wing.

The superiority of the strake wing is slightly reduced when applying high-lift flap systems and/or spanwise blowing, but the strake wing remains to be the superior design.

IV. 2. Effect of Spanwise Blowing at Extreme Incidences $\alpha \leq 90^\circ$

This second test phase was carried out in the 8m ϕ tunnel S1, ONERA Modane, and is part of a programme of cooperation between O.N.E.R.A. and MBB. The same model and instrumentation was used, the wing additionally equipped with tip accelerometers and strain gauges for wing root torsional moments, to get some further information about the configuration's buffet behaviour.

Taking in account the aforementioned superiority of the strake wing at high angles-of-attack, only this configuration was tested applying spanwise blowing. An additional justification for that is given by the expected 97% regain of thrust due to the 75° swept nozzles as compared to the more lateral blowing nozzles for the basic configuration.

A photo of the configuration selected is given in Fig. 14, showing the sting mounted pilot model in the wind tunnel S1 of ONERA, Modane.

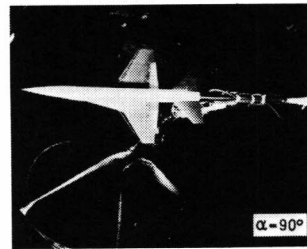


FIG. 14 PILOT MODEL IN TUNNEL S1, ONERA, MODANE (TEST SECTION 8m ϕ)

IV. 2.1 Aerodynamic effects

The effect of spanwise blowing in the angle-of-attack regime $\alpha = 0 + 90^\circ$ is demonstrated for lift, pitching moment and drag data in Fig. 15.

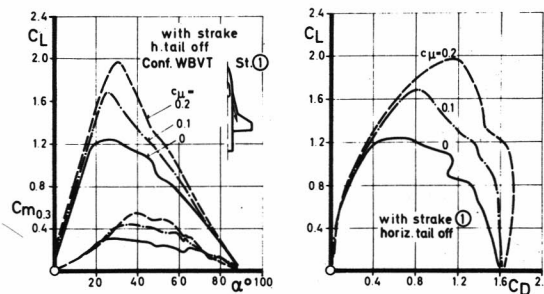


FIG. 15 EFFECT OF SPANWISE BLOWING IN THE ANGLE OF ATTACK REGIME $\alpha = 0 + 90^\circ$

Blowing is affecting lift and pitching moment data up to $\sim 70^\circ$ incidence, whereby the additional lift, induced by the jet-vortex interaction, is positioned successively forward until it breaks near 70° angle-of-attack.

Consequently trimming is alleviated by increased momentum coefficients c_{μ} as shown in Fig. 16 for the lift polar and in Fig. 17 for the tail trim settings.

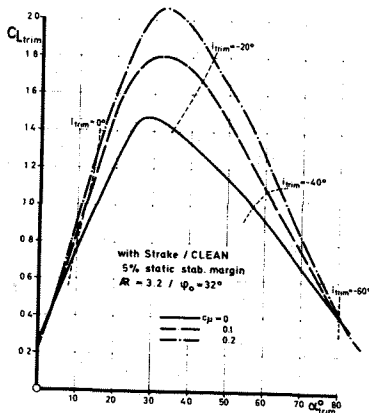


FIG. 16 TRIMMED LIFT POLARS FOR DIFFERENT BLOWING INTENSITIES

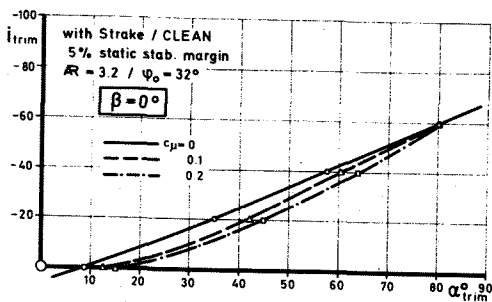


FIG. 17 HORIZONTAL TAIL TRIM ANGLES AS AFFECTED BY ANGLE OF ATTACK AND SPANWISE BLOWING

At a.o.a. below the stall the increased trimmed incidence for constant tail setting is traced back on a slightly increased downwash on the low positioned horizontal tail. For poststall a.o.a. the main effect is deduced from the wing-body center of pressure movement forward, as stated above. For a 5% static stability margin the configuration is longitudinally trimmable by the fully rotating, all-moving horizontal tail. Trim characteristics are nearly linear (Fig. 17) for the complete a.o.a. regime $\alpha = 0 + 90^\circ$.

To get some insight into the buffet characteristics in the a.o.a. regime investigated, the wing was equipped with strain gauges to determine RMS data of the wing root bending and torsional moment.

Additionally two tip accelerometers were positioned at 25% and 65% tip chord. The results obtained with the different sensors all give the same basic information

as presented in Fig. 18 for the recorded wing root bending moment RMS data:

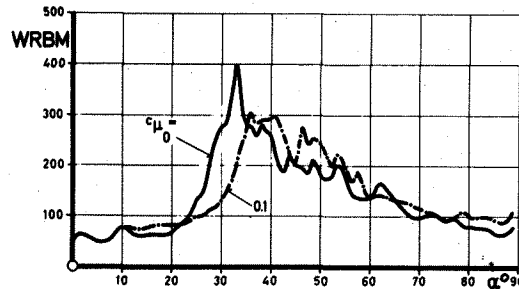


FIG. 18 EFFECT OF SPANWISE BLOWING ON BUFFET INTENSITY (RMS-DATA OF WING ROOT BENDING MOMENT OSCILLATION)

- o at low incidence spanwise blowing induces some additional slight disturbances
- o the angle of divergence is shifted to higher values, thus an increase of the buffet-onset lift ($CL_{c_{\mu}=0} = 1.2 / CL_{c_{\mu}=0.1} = 1.68$) of approximately 40% is found for $c_{\mu} = 0.1$.
- o generally peak loads are found at angles-of-attack slightly above maximum lift
- o despite of the higher static maximum lift of the blown wing, peak buffet intensities are reduced by spanwise blowing
- o with further increase of incidence buffet intensity varies approximately with the correspondent static lift developed by the respective configuration
- o at 90° a.o.a. the RMS data tend to end in the level of the basic low angle-of-attack data.

IV. 2.2 System integrated effects

Direct jet effects of the blowing system were not measured in the previous investigation. So the analysis was concentrated on indirect, jet induced aerodynamic responses, according to the applied method of testing. To establish the true merits of this blowing technique the total rating has to be considered, including engine thrust and jet reaction effects. This means, that we carefully have to watch the consequences of integrating this system into an aircraft. The following chapter will concentrate on some major factors involved when engine and thrust effects are taken in account additionally.

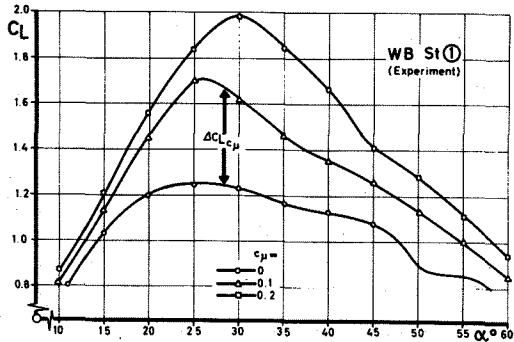


FIG. 19 EFFECT OF SPANWISE BLOWING ON WING LIFT

Recalling the experimentally found aerodynamic effects of spanwise blowing on lift production Fig. 19 gives an extract of Fig. 15. The lift increments developed by spanwise blowing are drawn out in the a.o.a. regime $\alpha = 10 + 60^\circ$ for momentum coefficients $c_\mu = 0/0.1/0.2$.

This lift increment $\Delta CL_{C\mu}$ is causing a drag increment $\Delta CD_{C\mu}$ for fixed angle-of-attack. Plotting these two increments $\Delta CL_{C\mu}$ versus $\Delta CD_{C\mu}$ gives the incremental polars depicted in Fig. 20.

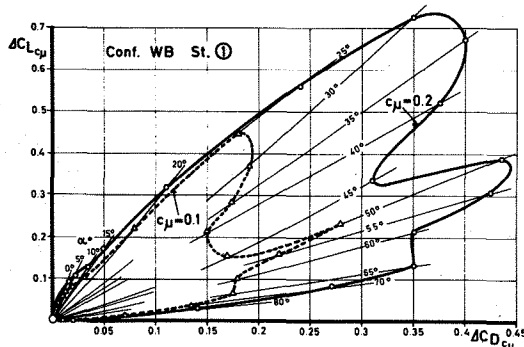


FIG. 20 EFFECT OF SPANWISE BLOWING ON DRAG POLARS; INCREMENTAL POLARS

Not taking in account the zero-lift drag (negligible for $\alpha > 10^\circ$) lines of constant angle-of-attack are represented by rays through the origin. This is derived from the type of flow characterized by leading edge separation, hence $\Delta C_{W C\mu} = K \cdot \Delta C_{A C\mu} \cdot \tan \alpha$ or

$$\frac{\Delta C_A}{\Delta C_W} c_\mu = \frac{1}{K} \cotan \alpha.$$

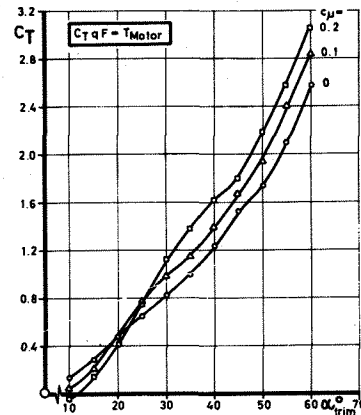


FIG. 21 REQUIRED ENGINE THRUST COEFFICIENT C_T FOR BALANCED FLIGHT

To balance the total drag for level flight, a certain amount of engine thrust C_T is required (Fig. 21).

The thrust component produced by the nozzles acting for spanwise blowing (nozzle position at 10% root chord of strake wing, jet axis swept back 75°) is not included in this coefficient, as can be seen at low angles-of-attack for different momentum coefficients. Then the blowing jet thrust component starts to take charge of providing the necessary propulsion ($C_T = 0 =$ tail nozzle thrust coefficient). Hence we consider the blowing jet to be produced by an auxiliary power unit, thus avoiding the problem of amplified tapping losses involved, when one tries to take bleed air from the relatively delicate high pressure compressor of the main engine (taking i.e. 5% of mass flow would result in about 30% thrust loss at the tail nozzle for an examined contemporary power plant).

Engine + APU thrust are producing lift components which are plotted in Fig. 22 as effective lift increments ΔCL_{eff} versus angle-of-attack.

This summed up increment can be split into parts, as shown in Fig. 22:

- o the first contribution is given by the tilted motor thrust for zero-blowing cases, denoted as $(\Delta CL_{TM})_{c_\mu=0}$
- o the second term is related to the application of spanwise blowing and comprises the direct lift component of the blowing nozzles ΔCL_{TB} plus a further increment of lift $(\Delta CL_{TM})_{c_\mu}$ produced by the motor

(= tail nozzle), to compensate for the additional drag, produced by the induced lift increment at a fixed a.o.a. (see incremental drag polar of Fig. 20).

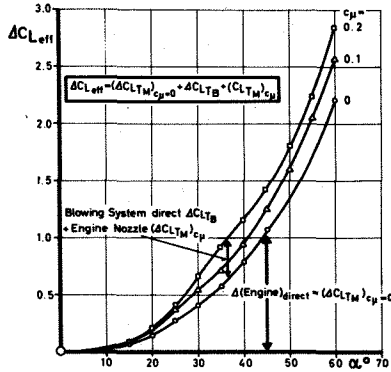


FIG. 22 LIFT-COMPONENTS DUE TO THRUST (ENGINE AND BLOWING JET)

Now having established all the components in terms of lift and drag for the integration of the blowing system, Fig. 23 summarizes the aerodynamic and thrust effects as total "effective lift" CL_{eff} .

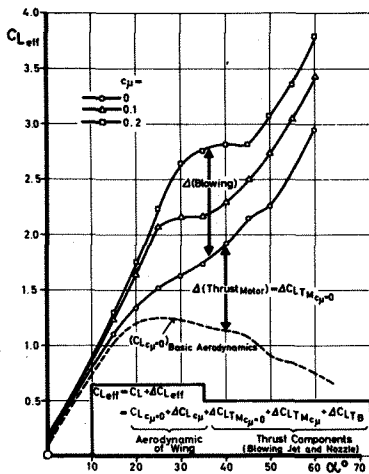


FIG. 23 TOTAL EFFECTIVE LIFT INCLUDING ENGINE AND BLOWING JET EFFECTS

The build up is in analogy to Fig. 22, thus deviding again in basic aerodynamic effects and basic thrust effects ($c_{\mu} = 0$) and then adding direct and indirect com-

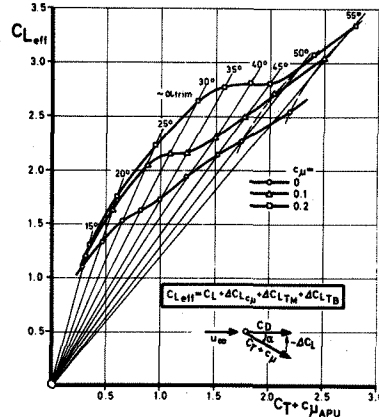


FIG. 24 EFFECTS OF SPANWISE BLOWING ON EFFECTIVE POLAR

ponents due to spanwise blowing. It can be seen easily that with increasing a.o.a. engine thrust starts to play the dominant role in producing the total effective lift vector.

Replacing aerodynamic lift by this effective total lift CL_{eff} , and using engine thrust c_T plus APU thrust c_{μ} instead of drag, results in the "effective polar", presented in Fig. 24. The ratio $CL_{eff} / (c_T + c_{\mu})$ is giving a measure of the expense of motorization paid for a certain amount of lifting force (at high angles-of-attack) and is an equivalent to the well known conventional lift/drag ratio.

Fig. 24 was used for the next two figures to extract the increments due to spanwise blowing and to establish the total efficiency of this technique.

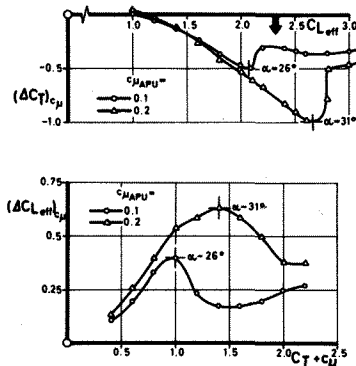


FIG. 25 NET EFFECTS OF SPANWISE BLOWING
 • REDUCTION OF REQUIRED THRUST FOR CONSTANT TOTAL LIFT (top)
 • ADDITIONAL LIFT FOR CONSTANT TOTAL THRUST SETTING (bottom)

In Fig. 25 (top) the reduction of total thrust coefficient is plotted, taking the differences $(c_T + c_{\mu})_{c_{\mu}} - c_{T,c_{\mu}=0}$ for const.

effective lift, whilst in Fig. 25 (bottom) the increment in total effective lift $(C_{Leff})_{C_{\mu}} - (C_{Leff})_{C_{\mu}=0}$ was taken for constant degrees of motorization $(C_T + C_{\mu})$.

The efficiency curves $\Delta C_L / C_{\mu}$ of Fig. 26 were derived from Fig. 19 (aerodynamic lift increment) and from Figures 23 and 24 for the integrated system, now taking the ratio at constant angles-of-attack and comparing the factors $\Delta C_L / C_{\mu}$ with the effectivity of a hovering jet. Integration of the technique develops amplified efficiency factors relative to the pure aerodynamic improvements thus demonstrating the qualification of this simple technique especially for highly maneuverable aircraft at low speeds.

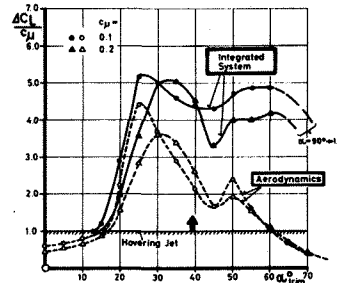


FIG. 26 EFFICIENCY FACTORS OF SPANWISE BLOWING
 • AERODYNAMIC EFFICIENCY
 • INTEGRATED SYSTEM EFFICIENCY

V. REFERENCES

- DAS A.
 Vorversuche über die Wirbelbildung bei Tragflügeln von kleinem Seitenverhältnis
 DFL-Bericht Nr. 099 1960
- WERLE H.
 Sur l'éclatement des tourbillons d'apex d'une aile delta aux faibles vitesses
 La Recherche Aéronautique No.74 1960
- DAS A.
 Versuche über die Wirbelbildung bei Deltaflügeln von kleinem Seitenverhältnis
 DFL-Bericht Nr. 0137 1961
- LUDWIG H.
 Zur Erklärung der Instabilität der über angestellten Deltaflügeln auftretenden freien Wirbelkerne
 AVA-Bericht 1961
- HUMMEL D.
 Untersuchungen des Strömungsfeldes, insbesondere des Aufplatzens der Wirbelkerne, an einem schlanken Deltaflügel
 DFL-Bericht Nr. 0196 1963
- HUMMEL D.
 Untersuchungen über das Aufplatzen der Wirbel an schlanken Deltaflügeln
 Z. Flugwissenschaften 1965
- POLHAMUS E.C.
 A concept of the vortex lift of sharp-edge delta wings based on a leading-edge-suction analogy
 NASA TN D-3767 1966
- SACHER P. / PFANZEDER D.
 Nicht-lineare Theorie für Flügel kleiner Streckung:
 Voruntersuchung im Wasserkanal
 EWR Nr. 454-69 1969
- WENTZ W.H. Jr.
 Vortex Breakdown on Slender Sharp-Edged Wings
 J.A. Vol. 8 No. 3 1969
- DIXON C.J.
 Lift augmentation by lateral blowing over a lifting surface
 AIAA No. 69-193 1969
- CORNISH J.J. III
 High lift application of spanwise blowing
 ICAS Paper No. 70-09 1970
- DIXON C.J.
 Lift and control augmentation by spanwise blowing over trailing edge flaps and control surfaces
 AIAA Paper No. 72-781 1972

- STAUDACHER W.
Verbesserung der Manöverleistungen im hohen Unterschall
MBB-Bericht UFE896-72/
DGLR-72-126 1972
- BRADLEY R.G. / SMITH C.W. / BHATELEY I.C.
Vortex-lift prediction for complex wing planforms
J. Aircraft Vol. 10 No. 6 1973
- THEISEN J.G. / SCRUGGS R.M. / DIXON C.J.
Theoretical and experimental investigations of vortex lift control by spanwise blowing
LOCHHEAD-Georgia Report 1973
- STAUDACHER W.
Zum Einfluß von Flügelgrundriß-Modifikationen auf die aerodynamischen Leistungen von Kampfflugzeugen
MBB-Bericht UFE1033-73/
DGLR-73-71 1973
- ZECH A./STAUDACHER W./BRETTHAUER N.
Untersuchungen im Unterschall an Flügeln mit Strakes für Kampfflugzeuge
MBB-Bericht UFE1019 1973
- BRADLEY R.G. / SMITH C.W. / WRAY W.O.
An experimental investigation of leading-edge vortex augmentation by blowing
NASA CR-132515 1974
- CAMPBELL J.F.
Effects of spanwise blowing on the pressure field and vortex-lift characteristics of a 44° swept trapezoidal wing
NASA TN D-7907 1975
- BRADLEY R.G. / WHITTEN P.D. / WRAY W.O.
Leading-edge vortex augmentation in compressible flow
AIAA Paper Nr. 75-124 1975
- KNORR G.
Experimenteller Vergleich zweier Ausblas-konzepte am Modell eines leichten STOL-Flugzeuges
T.U. Braunschweig, Studienarbeit 1975
- BAUMERT W.
Druckverteilungs-Messungen am Prinzipmodell Flügel mit Strake bei unsymmetrischer Anblasung
DFVLR IB 157-75 A17 1975
- JENKINS M.W.M. / MEY R.T.
A large-scale low-speed tunnel test of a canard configuration with spanwise blowing
AIAA Paper No. 75-994 1975
- CAMPBELL J.F.
Augmentation of vortex lift by spanwise blowing
AIAA Paper No. 75-993 1975
- HÜNECKE K. / KRAHL H.
Grundsatz-Untersuchungen über spannweitiges Ausblasen
VFW-FOKKER Bericht Ef-626 1975/1976
- PARKER A.G.
Aerodynamic characteristics of slender wings with sharp leading edge - a review
J.A. Vol. 13 No. 3 1976
- NUGMANOV H. Kh.
Experimental study of spanwise airjet influence on wing aerodynamic characteristics
Izvestiya VUZ. Aviatsionnaya Tekhn. 1976
- WULF R. / BÖDDENER W.
Kraftmessungen an einem Pilotmodell, Einfluß von spannweitigem Blasen an Strakes, Flügel oder Hinterkantenklappen - Ergebnislisten -
DFVLR-Bericht IB 157-76 A30 1976
- STAUDACHER W. / HÜNECKE K.
Flügel mit und ohne Strakes im Post-Stall-Bereich
Gemeinschaftsber. MBB-UFE1300/VF Ef-652
ZTL 1976
- STAUDACHER W.
The effects of jets, wakes and vortices on lifting surfaces
AGARD FDP RTD/MBB-UFE-AERO-MT-263 1976
- KRUPPA E.W.
A wind tunnel investigation of the KASPER vortex concept
AIAA Paper No. 77-310 1977
- STAUDACHER W./BÖDDENER W./WULF R.
Grundsätzliche Untersuchungen über spannweitiges Ausblasen und stabilisierten Wirbelauftrieb
Gemeinschaftsbericht MBB-UFE1320/
DFVLR IB 157-77 A25 ZTL 1977
- STAUDACHER W.
Flügel mit kontrollierter Ablösung
MBB-UFE1343(Ö)/DGLR Nr. 77-028 1977
- POISSON-QUINTON Ph.
Slender wings for civil and military aircraft
8th Theodore v. Karman Lecture 1978